Experimental Estimation of Entanglement at the Quantum Limit

Giorgio Brida,[1] Ivo Pietro Degiovanni,[1] Angela Florio,[1,2] Marco Genovese,[1] Paolo Giorda,[3] Alice Meda,[1] Matteo G. A. Paris,[4,5] and Alexander Shurupov[6,1,7]

[1]*INRIM, I-10135, Torino, Italy*
[2]*Dipartimento di Fisica, Università di Bari, I-70126 Bari, Italy*
[3]*ISI Foundation, I-10133 Torino, Italy*
[4]*Dipartimento di Fisica, Università degli Studi di Milano, I-20133 Milano, Italy*
[5]*CNISM, UdR Milano, I-20133 Milano, Italy*
[6]*Dipartimento di Fisica, Politecnico di Torino, I-10129 Torino, Italy*
[7]*Faculty of Physics, Moscow State University, 119992, Moscow, Russia*

(Received 24 July 2009; published 8 March 2010)

Entanglement is the central resource of quantum information processing and the precise characterization of entangled states is a crucial issue for the development of quantum technologies. This leads to the necessity of a precise, experimental feasible measure of entanglement. Nevertheless, such measurements are limited both from experimental uncertainties and intrinsic quantum bounds. Here we present an experiment where the amount of entanglement of a family of two-qubit mixed photon states is estimated with the ultimate precision allowed by quantum mechanics.

DOI: 10.1103/PhysRevLett.104.100501 PACS numbers: 03.67.Mn, 03.65.Ta, 42.50.Xa

Introduction.—Entanglement is the central resource of quantum information processing and the precise characterization of entangled states is a crucial issue for the development of quantum technologies. In turn, quantification and detection of entanglement have been extensively investigated, see [1–3] for a review, and different approaches have been developed to extract the amount of entanglement of a state from a given set of measurement results [4–7]. Of course, in order to evaluate the entanglement of a quantum state one may resort to full quantum state tomography [8] that, however, becomes impractical in higher dimensions and may be affected by large uncertainty [9]. Other methods, requiring a reduced number of observables, are based on visibility measurements [10], nonlocality tests [11,12], entanglement witnesses [13–15] or are related to Schmidt number [16,17]. Many of them found an experimental application [18–21], also in the presence of decoherence effects [22,23].

Any quantitative measure of entanglement corresponds to a nonlinear function of the density operator and thus cannot be associated to a quantum observable. As a consequence, ultimate bounds to the precision of entanglement measurements cannot be inferred from uncertainty relations. Any procedure aimed to evaluate the amount of entanglement of a quantum state is ultimately a parameter estimation problem, where the value of entanglement is indirectly inferred from the measurement of one or more proper observables [24]. An optimization problem thus naturally arises, which may be properly addressed in the framework of quantum estimation theory [25–28], which provides analytical tools to find the optimal measurement and to derive ultimate bounds to the precision of entanglement estimation.

Preliminaries.—Suppose one has a family of quantum states ϱ_ϵ labeled by the value of entanglement, say negativity [1,29] $\epsilon = \|\varrho_\epsilon^\theta\|$, where θ denote partial transposition and $\|\cdots\|$ trace norm, and wants to estimate ϵ from the outcomes N repeated measurements of the (generalized) observable described by a positive operator-valued measure (POVM) Π_x, $\sum_x \Pi_x = \mathbb{1}$. Any inference strategy amounts to find an *estimator*, i.e., a map $\hat{\epsilon}(\chi)$ from the experimental sample to the parameter space. According to the Cramer-Rao theorem the precision of any estimation procedure, i.e., the variance of any unbiased estimator based on the measurement of Π_x, is bounded by the inequality $\mathrm{Var}(\hat{\epsilon}) \geq [NF_\epsilon]^{-1}$, where $F_\epsilon = \sum_x p(x|\epsilon) \times [\partial_\epsilon \ln p(x|\epsilon)]^2$ is the Fisher information and $p(x|\epsilon) = \mathrm{Tr}[\varrho_\epsilon \Pi_x]$ is the conditional probability of getting the outcome x when the actual value of entanglement is ϵ. Upon maximizing the Fisher information over all the possible quantum measurements we arrive at the quantum Fisher information (QFI) $H_\epsilon = \mathrm{Tr}[L_\epsilon^2 \varrho_\epsilon]$ expressed in terms of the symmetric logarithmic derivative L_ϵ, i.e., the self-adjoint operator defined by $\partial_\epsilon \varrho_\epsilon = \frac{1}{2}(L_\epsilon \varrho_\epsilon + \varrho_\epsilon L_\epsilon)$. We have $F_\epsilon \leq H_\epsilon$ and the ultimate bounds to precision are determined by the quantum Cramer-Rao bound (QCRB) $\mathrm{Var}(\hat{\epsilon}) \geq [NF_\epsilon]^{-1} \geq [NH_\epsilon]^{-1}$. The meaning of the QCRB is that quantum mechanics does not allow entanglement estimation with arbitrary precision. In turn, QCRB represents the ultimate bound to the precision, at fixed number measurements, of *any* procedure aimed to estimate the amount of entanglement of a state of the family ϱ_ϵ. For a multiparameter family of states one evaluates the QFI matrix $\boldsymbol{H}_{\mu\nu} = \mathrm{Tr}[\frac{1}{2}(L_\mu L_\nu + L_\nu L_\mu)\varrho]$ and the ultimate bound to estimation of entanglement at fixed value of the other parameters may be written as above with the replace-

ment $H_\epsilon^{-1} \rightarrow \boldsymbol{H}_{\epsilon\epsilon}^{-1}$ where $\boldsymbol{H}^{-1}$ is the inverse of the QFI matrix.

In order to optimally estimate entanglement we need (i) a measurement with Fisher information $F_\epsilon = H_\epsilon$ equal to the QFI and (ii) an estimator saturating the Cramer-Rao bound [30]. In [24], bounds to precision have been evaluated for several classes of pure and mixed quantum states. Here we demonstrate experimentally for the first time that optimized correlations measurements allow for the estimation of entanglement with the ultimate precision imposed by quantum mechanics. In particular, we present the results of an experiment to estimate the amount of entanglement (negativity) of two-qubit photon states. This represents a substantial advance, paving the way for further progresses. In fact, with a suitable choice of correlation measurements one can devise a procedure to optimally estimate entanglement for a generic class of two-photon entangled states.

Experimentals.—The family of entangled states we are dealing with is made of polarization entangled photon pairs obtained by coherently superimposed type-I parametric down-conversion (PDC) generated in two beta-Barium Borate (BBO) crystals [18]. The experimental setup is schematically depicted in Fig. 1. A continuous wave argon pump laser beam with wavelength $\lambda = 351$ nm is filtered with a dispersion prism and then passes through a Glan-Thompson prism that selects a horizontal polarization. A half-wave plate WP0 rotates the polarization by the angle ϕ, which in turn determines the amount of entanglement in the output state. PDC light is generated by two thin type-I BBO crystals ($l = 1$ mm), positioned with the planes that contain optical axes orthogonal to each other. PDC occurs only in crystal 1 (2) if the polarization of the pump beam is horizontal (vertical).

The crystals are cut for collinear frequency degenerate phase matching at working wavelength and the phase shifts due to ordinary and extraordinary path in the crystals are compensated by rotating the quartz plates (QP). The pump is stopped by a filter (UVF), and the biphoton field is split on a nonpolarizing 50-50 beam splitter (BS). The measurement stage consists in projecting the beams on vertical polarizers after passing through half-wave plates (WP1, WP2). After spectral selection by interference filters (IF)

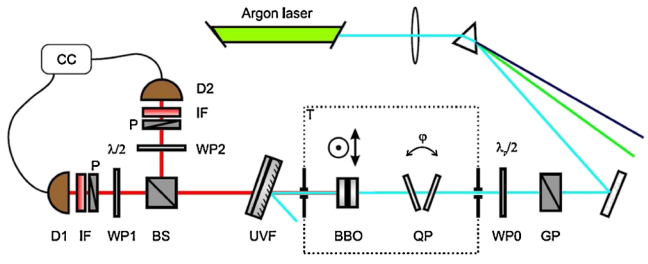

FIG. 1 (color online). Experimental setup to generate polarization entangled photon pairs with variable entanglement and estimate its value with the ultimate precision allowed by quantum mechanics.

centered at the degeneracy 702 nm (FWHM = 3 nm), biphotons are focused on commercial single photon detectors (D1, D2). The detectors' outputs are registered by means of a coincidence scheme (CC) with a window time of 1 ns. To maintain stable phase-matching conditions, BBO crystals and QP are placed in a closed box, which is kept heated at a fixed temperature by a feedback loop control system.

Family of entangled states.—In ideal conditions our setup generates entangled pairs of the form $|\psi_\phi\rangle = \cos\phi|HH\rangle + \sin\phi|VV\rangle$ (H and V denoting horizontal and vertical polarizations, respectively). The angle ϕ may be tuned by rotating the pump polarization with the half-wave plate WP0. Overall, the output states are described by the family of density matrices $\varrho_\epsilon = p|\psi_\phi\rangle\langle\psi_\phi| + (1-p)D_\phi$, where the small fraction $(1-p)$ of a separable mixture $D_\phi = \cos^2\phi|HH\rangle\langle HH| + \sin^2\phi|VV\rangle\langle VV|$ is added to take into account the decoherence mechanisms occurring in the experimental setup. These are mostly due to fluctuations of the relative phase between the two polarization components, which themselves derive from residual temperature fluctuations. The model has been validated by two-qubit polarization tomography [31,32] providing full state reconstruction. By tuning ϕ with WP0 one may generate states ϱ_ϵ with different negativity $\epsilon = p\sin 2\phi$ and purity $\mu = \mathrm{Tr}[\varrho_\epsilon^2] = 1 - (1-p^2)\sin 2\phi$. Upon inverting these relations and expressing the family of states in terms of ϵ and μ or p we may evaluate the QFI matrix. The QCRB turns out to be a function of ϵ only, $\boldsymbol{H}_{\epsilon\epsilon}^{-1} = (1-\epsilon^2)^{-1}$.

Estimation of entanglement.—We now describe our detection strategy and show it allows entanglement estimation with precision saturating the QCRB independently on the purity. The measurement setup allows for the projection measurements $\{\Pi_x\}$ onto following two-qubit states:

$$\Pi_x(\alpha,\beta) = \left|\alpha + s\frac{\pi}{2}\right\rangle\left\langle\alpha + s\frac{\pi}{2}\right| \otimes \left|\beta + s'\frac{\pi}{2}\right\rangle\left\langle\beta + s'\frac{\pi}{2}\right|$$

where $x = \{s + 2s'\}$, $s, s' = 0, 1$. As already pointed out before, the polarization angles α, β are set by means of vertical polarizers and WP1 and WP2 mounted on precision rotation stages with high resolution and fully motor controlled. Let us first illustrate precision analysis assuming the generation of the pure states $|\psi_\phi\rangle$. In this case the estimation of the negativity $\epsilon = \sin 2\phi$ reduces to a measurement of coincidence rates in a two-particle interferometer setting [10]. Indeed, upon inspecting the expression of the probabilities $p_x(\epsilon;\alpha,\beta) = \langle\psi_\phi|\Pi_x(\alpha,\beta)|\psi_\phi\rangle$, $x = 0, 1, 2, 3$ one finds out that unbiased estimators for the negativity can be written as $\hat{\epsilon} = V(\alpha,\beta)\csc 2\alpha \csc 2\beta - \cot(2\alpha)\cot(2\beta)$, where $V(\alpha,\beta) = (k_0 - k_1 - k_2 + k_3)/K$ is the two-qubit quantum correlation (QC) built in terms of

the recorded coincidence counts $k_x \equiv k_x(\alpha, \beta)$, $K = \sum_x k_x$, $x = 0, 1, 2, 3$. The Fisher information of the measurement is given by $F_\epsilon = \sum_x p_x(\epsilon; \alpha, \beta) \times [\partial_\epsilon \log p_x(\epsilon; \alpha, \beta)]^2$ and it equals the QFI, H_ϵ for the estimation of negativity. Our QC estimator saturates the QCRB for $\alpha, \beta = \pm\pi/4$ and thus $\hat{\epsilon} = V(\pm\pi/4, \pm\pi/4)$, which can be measured with the above experimental setup, represent optimal estimators of entanglement. In our implementation we set $\alpha = -\pi/4$ and $\beta = \pi/4$ independently on ϕ. In each run $j = 1, \ldots, M = 30$ one records the vector $\mathbf{k}_j = \{k_{0,j}, k_{1,j}, k_{2,j}, k_{3,j}\}$ of coincidence as measured for the given set of parameters by the coincidence circuit during a single time window (10 seconds). For large values of the total number of coincidences $K_j = \sum_x k_{x,j}$, the expected value of the coincidence rate $k_{x,j}(\alpha, \beta)/K_j$ converges to the probability $p_x(\epsilon; \alpha, \beta)$ and the optimal estimator can be realized in terms of the coincidences' vector: $\hat{\epsilon} \equiv \hat{\epsilon}(\mathbf{k_j})$. We first observe that for finite K_j's the uncertainty in the estimation of entanglement are mostly due to fluctuations δk_x in the coincidence counts $k_{x,j}$ around their average values $\langle k_x \rangle = \sum_j k_{x,j}/M$. Thus, we want to establish under which conditions on the fluctuations δk_x the variance of the estimator $\hat{\epsilon}(\mathbf{k_j})$ saturates the QCR bound. Using standard uncertainty propagation with the derivatives $\partial_x \equiv \partial/\partial k_x$ evaluated for $k_x \equiv \langle k_x \rangle$, and assuming independence among fluctuations at different angles, we have $\mathrm{Var}(\hat{\epsilon}) = \sum_x |\partial_x \hat{\epsilon}|^2 \delta k_x^2 = 4[(\langle k_0 \rangle + \langle k_3 \rangle)^2(\delta k_1^2 + \delta k_2^2) + (\langle k_1 \rangle + \langle k_2 \rangle)^2(\delta k_0^2 + \delta k_3^2)]/\langle K \rangle^4$. If we now assume that the counting processes have a Poissonian statistics, i.e. $\delta k_x^2 = \mathrm{Var}(k_x) = \langle k_x \rangle$, then it is straightforward to prove that

$$\mathrm{Var}\,(\hat{\epsilon}) = 4(k_0 + k_3)(k_1 + k_2)/\langle K \rangle^3 = (1 - \hat{\epsilon}^2)/\langle K \rangle;$$

i.e., QC measurements allow for optimal estimation of entanglement with precision at the quantum limit. Since the QCRB may be written as $\mathrm{Var}(\hat{\epsilon}) \geq (1 - \epsilon^2)/N$ for a wide range of two-qubit families of states [24], the above calculations suggest that this is a general result. In other words, given a source emitting polarization two-qubit states with coincidence counting statistics satisfying the Poissonian hypothesis, then the experimental setup of Fig. 1 allows for optimal estimation of entanglement at the quantum limit by means of a QC estimator.

This can be extended to the case of output states ϱ_ϵ. In fact, upon evaluating the probabilities $p_x(\epsilon; \alpha, \beta) = \mathrm{Tr}[\varrho_\epsilon \Pi_x(\alpha, \beta)]$, one sees that $\hat{\epsilon} = V(-\pi/4, \pi/4)$ is still an optimal (unbiased) estimator of entanglement. We have thus collected $M = 30$ repeated acquisitions of coincidence vector $\boldsymbol{k}_j = \{k_{0j}, k_{1j}, k_{2j}, k_{3j}\}$, then we have randomized the composition of $\boldsymbol{k}_j$ over the sequence of measurements to avoid accidental correlations, and finally we have estimated entanglement as the sample mean $\langle \hat{\epsilon} \rangle = \sum_j \hat{\epsilon}(\boldsymbol{k}_j)/M$. The corresponding uncertainty has been evaluated by the sample variance $\mathrm{Var}(\hat{\epsilon}) = \sum_j [\hat{\epsilon}(\boldsymbol{k}_j) - \langle \hat{\epsilon} \rangle]^2/(M - 1)$. In order to compare the estimated value of entanglement with the actual one we need to estimate also the additional parameter p, quantifying the amount of mixing introduced by decoherence processes. An unbiased estimator $\hat{p}$ for this parameter may be obtained by measuring QC with a different set of angles, e.g., upon collecting the coincidences $\mathbf{r_j} \equiv \mathbf{k_j}(\alpha = \beta = \mathbf{0})$ to form $\hat{p}(\boldsymbol{r}_j, \boldsymbol{k}_j) = \frac{1}{2}\hat{\epsilon}(\boldsymbol{k}_j) R_j/\sqrt{r_{3,j}(1 - r_{3,j})}$, where $R_j = \sum_x r_{x,j}$ is the total number of coincidences with the four orientations $\alpha, \beta = 0, \pi/2$. The actual (''true'') value of negativity is then inferred as $\epsilon_x = \langle \hat{p} \rangle \sin 2\phi$, i.e., using the knowledge of the rotation angle of the wave plate WP0 and the estimation of the mixing parameter.

Results.—In Fig. 2 we show the estimated value of entanglement as a function of the actual one for the following values of the WP0 rotation angle and mixing $\phi = 10°$, $15°$, $20°$, $28°$, $40°$, $42°$, $45°$, $\langle \hat{p} \rangle = 0.85, 0.88, 0.88, 0.85, 0.92, 0.93, 0.97$. The uncertainty bars on $\langle \hat{\epsilon} \rangle$ denote the quantity $\sqrt{\mathrm{Var}(\hat{\epsilon}) \times \langle K \rangle}$, i.e., the square root of the sample variance multiplied by the average number of total coincidences $\langle K \rangle$. This is in order to allow a direct comparison with the Cramer-Rao bound in terms of the inverse of the Fisher information (the gray area). Uncertainty bars on the abscissae correspond to fluctuations $\delta\epsilon_t = \sqrt{\mathrm{Var}(\hat{p})} \sin 2\phi$ in the determination of ϵ_t, due to fluctuations in the estimation of the mixing parameter. As it is apparent from the plot, entanglement is estimated with precision at the quantum limit for any value of the rotation angle ϕ. Notice that this conclusion is robust against the fact that the statistics is not exactly Poissonian: in the left panel of Fig. 3 we show the Fano factor for the four recorded coincidence counts k_j and the seven values of ϕ employed in the experiment. We have also performed full polarization tomography [31,32] of the state evaluating negativity with the reconstructed

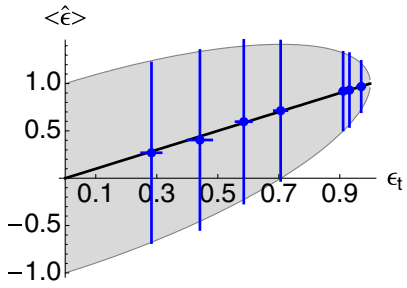

FIG. 2 (color online). Estimation of entanglement at the quantum limit. The plot shows the estimated value of entanglement $\langle \hat{\epsilon} \rangle$ as a function of the actual one ϵ_t. The uncertainty bars on $\langle \hat{\epsilon} \rangle$ denote the quantity $\sqrt{\mathrm{Var}(\hat{\epsilon}) \times \langle K \rangle}$, i.e., the square root of the sample variance multiplied by the average number of total coincidences $\langle K \rangle$. The gray area corresponds to values within the inverse of the Fisher information $\epsilon_t \pm H_{\epsilon_t}^{-1/2}$. Uncertainty bars on the abscissae correspond to fluctuations $\delta\epsilon_t = \sqrt{\mathrm{Var}(\hat{p})} \sin 2\phi$ in the determination of ϵ_t, due to fluctuations in the estimation of the mixing parameter.

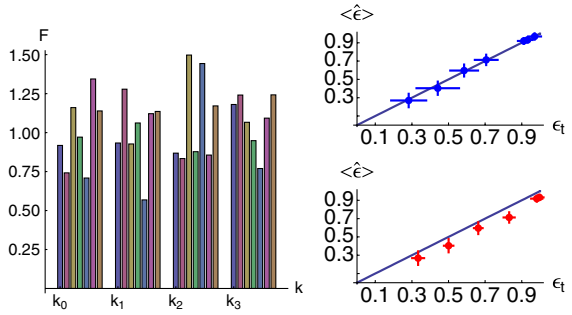

FIG. 3 (color online). Left: Fano factors of the coincidence counts k_j, $j = 0, 1, 2, 3$. Each group contains the Fano factor for the seven values of ϕ reported in the text. Right: estimated value of entanglement as a function of the actual one assuming, for the description of the output signals, the families ϱ_ϵ (top plot) and ϱ'_ϵ (bottom plot). The uncertainty bars correspond to the 3σ confidence interval.

matrix elements results, obtaining a more noisy determination of entanglement.

Besides full state reconstruction, our statistical model ϱ_ϵ may be checked for consistency on the basis of the recorded data themselves. Results indicate that other possible models to describe decoherence of our family of states are ruled out as they cannot fit the experimental sample. As for example, if one tries to describe the output from our source by the family of (depolarized) Werner states $\varrho'_\epsilon = p|\psi_\phi\rangle\langle\psi_\phi| + \frac{1}{4}(1-p)\mathbb{1}\otimes\mathbb{1}$, then one sees from the expression of the coincidence probability $p'_t(\epsilon;\alpha,\beta) = \mathrm{Tr}[\varrho'_\epsilon \Pi_t(\alpha,\beta)]$ that unbiased estimators for the mixing parameters and the negativity may be expressed as $\hat{p}' = V(0,0)$, $\hat{\epsilon}' = -\frac{1}{2} + \frac{1}{2}V(0,0) + V(-\pi/4,\pi/4)$. These may be written in terms of the coincidence vectors $\mathbf{k}$ and $\mathbf{r}$ as $\hat{p}'(\boldsymbol{r}_j) = (r_{r0,j} - r_{1,j} - r_{2,j} + r_{3,j})/R_j$ and $\hat{\epsilon}'(\mathbf{r}_j,\mathbf{k}_j) = -\frac{1}{2} + \frac{1}{2}\hat{p}'(\boldsymbol{r}_j) + (k_{0,j} - k_{1,j} - k_{2,j} + k_{3,j})/K_j$. Upon evaluating the corresponding sample means and variances one realizes that the model is incompatible with the observed data. This is illustrated in the right panel of Fig. 3 where we report the estimated value of entanglement as a function of the actual one assuming, for the description of the output signals, the families ϱ_ϵ (top plot) and ϱ'_ϵ (bottom plot). Here the uncertainty bars denote the 3σ confidence interval and thus it is apparent that ϱ'_ϵ cannot fit the data.

Conclusions.—We have suggested and demonstrated a measurement scheme based on quantum correlation measurements to optimally estimate entanglement for a family of two-photon entangled states. Our procedure is self-consistent and allows estimating the amount of entanglement with the ultimate precision imposed by quantum mechanics. With a suited choice of correlation measurements, our results may be extended to a generic class of two-photon entangled states. The statistical reliability of our method suggests a wider use in precise monitoring of external parameters assisted by entanglement.

This work has been supported in part by MIUR (PRIN 2007FYETBY), Regione Piemonte (E14), "San Paolo Foundation", and NATO (CBP.NR.NRCL.983251). M. G. A. P. and P. G. thank Marco Genoni for several useful discussions.

[1] R. Horodecki *et al.*, Rev. Mod. Phys. **81**, 865 (2009).
[2] O. Gühne and G. Toth, Phys. Rep. **474**, 1 (2009).
[3] R. Augusiak and M. Lewenstein, Quant. Info. Proc. **8**, 493 (2009).
[4] P. Lougovski and S. J. Van Enk, arXiv:0806.4165.
[5] H. Wunderlich and M. B. Plenio, J. Mod. Opt. **56**, 2100 (2009).
[6] J. Eisert *et al.*, New J. Phys. **9**, 46 (2007).
[7] K. Audenaert and M. B. Plenio, New J. Phys. **8**, 266 (2006).
[8] M. G. A. Paris and J. Rehacek, *Quantum state estimation*, Lect. Not. Phys. Vol. 649 (Springer, Berlin, 2004).
[9] G. M. D'Ariano *et al.*, Phys. Lett. A **195**, 31 (1994).
[10] G. Jaeger, M. A. Horne, and A. Shimony, Phys. Rev. A **48**, 1023 (1993).
[11] J. F. Clauser *et al.*, Phys. Rev. Lett. **23**, 880 (1969).
[12] R. Werner and M. Wolf, Quantum Inf. Comput. **1**, 1 (2001).
[13] M. Horodecki *et al.*, Phys. Lett. A **223**, 1 (1996).
[14] B. M. Terhal, Phys. Lett. A **271**, 319 (2000).
[15] O. Guhne *et al.*, Phys. Rev. A **66**, 062305 (2002).
[16] P. Facchi *et al.*, Int. J. Quantum. Inform.. **5**, 97 (2007).
[17] M. V. Fedorov *et al.*, J. Phys. B **39**, S467 (2006); P. A. Volkov *et al.*, Adv. Sci. Lett. **2**, 511 (2009). .
[18] M. Genovese, Phys. Rep. **413**, 319 (2005).
[19] M. Bourennane *et al.*, Phys. Rev. Lett. **92**, 087902 (2004).
[20] M. V. Fedorov *et al.*, Phys. Rev. Lett. **99**, 063901 (2007); Phys. Rev. A **77**, 032336 (2008).
[21] G. Brida *et al.*, Europhys. Lett. **87**, 64 003 (2009).
[22] S. P. Walborn *et al.*, Nature (London) **440**, 1022 (2006); A. R. R. Carvalho *et al.*, Phys. Rev. Lett. **98**, 190501 (2007).
[23] M. P. Almeida *et al.*, Science **316**, 579 (2007).
[24] M. G. Genoni, P. Giorda, and M. G. A. Paris, Phys. Rev. A **78**, 032303 (2008).
[25] C. W. Helstrom, Phys. Lett. A **25**, 101 (1967); C. W. Helstrom, *Quantum Detection and Estimation Theory* (Academic Press, New York, 1976).
[26] S. Braunstein and C. Caves, Phys. Rev. Lett. **72**, 3439 (1994); S. Braunstein *et al.*, Ann. Phys. (Leipzig) **247**, 135 (1996).
[27] D. C. Brody and L. P. Hughston, Proc. R. Soc. A **454**, 2445 (1998); **455**, 1683 (1999).
[28] Y. Bogdanov *et al.*, Phys. Rev. A **70**, 042303 (2004).
[29] I. Bengtsson and K. Zyczkowski, *Geometry of Quantum States* (Cambridge Press, Cambridge, UK, 2006).
[30] M. G. A. Paris, Int. J. Quantum. Inform. **7**, 125 (2009).
[31] K. Banaszek *et al.*, Phys. Rev. A **61**, 010304(R) (1999).
[32] D. F. V. James *et al.*, Phys. Rev. A **64**, 052312 (2001).